LOWLAND TECHNOLOGY INTERNATIONAL Vol. 2, No. 1, 47-64, June 2000
International Association of Lowland Technology (IALT), ISSN 1344-9656

# ESTIMATING WATER QUALITY OF THE ARIAKE SEA IN JAPAN USING LANDSAT-TM DATA —Evaluation of SDD and SST—

Thian Yew Gan[1], Koichiro Ohgushi[2] and Hiroyuki Araki[3]

ABSTRACT: Using Lowtran 7's estimated Rayleigh scattered and aerosol scattered radiance, the radiance reflected at the sea surface ($L_W(\lambda)$) is derived from the measured radiance of Landsat-TM images taken over the Ariake Sea. Then the $L_W(\lambda)$ averaged from 4 x 4 windows of pixels centered at 33 sampling sites was regressed against the observed Secchi disk depth (SDD) using linear regression algorithms. Results show that use of multi-date visible channels of Landsat-TM as the calibration data predicts more accurate and dependable SDD at the validation stage than use of single-date calibration data of Landsat-TM. This study confirms the feasibility of retrieving SDD (or turbidity/ suspended sediments) from Landsat-TM data. Limited experiments in the modeling sea surface temperature (SST) show the potential of predicting SST from the thermal channel (6) of Landsat-TM data using a simple linear regression.

## INTRODUCTION

The Landsat-TM (Thematic Mapper) data has been widely used to study water quality issues in small coastal bodies and lakes (e.g., Aranuvachapun and LeBlond, 1981; Tassan, 1987; Han et al., 1994; Pattiaratchi et al. 1994). Since the advent of space technology in recent decades, researchers have found great potential in evaluating non-point source pollution by remote sensing (e.g., Engman and Gurney, 1991). Besides, in view of the size of most major water bodies whose environmental well-beings are of important to us, and the cost of ground data collection, a feasible and economical approach to study the pollution problem of large water bodies is via satellite data. Regions of electromagnetic spectrum useful as indicators of water quality variables include visible, near infrared and infrared bands. The focus of this study is to estimate the water quality of the Ariake Sea using the Landsat-TM data.

## THE ARIAKE SEA

The Ariake Sea is a semi-closed L-shaped bay, about 90 km long, 20 m deep, and 1,700 $km^2$ in area (see Fig. 1). In the middle, it bends through almost $90^o$ and drains mostly through the Hayasaki Strait to the open sea. The Hayasaki Strait is only about 4 km wide but its depth ranges from 50 to 70 m. Major rivers flowing into the Ariake Sea are Chikugo, Yabe, Shirakawa, Midorikawa, Kase, Rokkaku and Honmyo rivers. These rivers carry much

1 Associate Professor, Department of Civil and Environment Engineering, University of Alberta, Edmonton T6G 2G7, CANADA.
2 Associate Professor, Department of Civil Engineering, Saga University, 1 Honjo, Saga 840-8502, JAPAN.
3 Associate Professor, Institute of Lowland Technology, Saga University, 1 Honjo, Saga 840-8502, JAPAN.
Note: Discussion on this paper is open until December 25, 2000.

sediment from the upstream basins and the tideland, which is visible to a distance of 6 to 7 km from the seashore during low tide.

The Ariake Sea has the largest tidal range in Japan, as much as 6 m in spring tide at Suminoe, its head bay. Water from the open sea enters into the Ariake Sea through the Hayasaki Straight and flows along its east coast, while water getting out of the bay is along its west coast. Sediments carried by several rivers into the bay have been mixed with suspended mud rolled up by the tide. These constituents have made a wide tideland in the northern coast of the Ariake Sea, which is very rich for many lives. This tideland was cultivated at first for agricultural use but people had started reclaiming land utilizing tidal effects about 700 years ago. After the Warring States period, when the Tokugawa Shogunate government starts, each feudal lord endeavored to make newly reclaimed rice fields. The Saga feudal clan was not its exception. These natural features of becoming tideland and artificial reclamations have formed vast lowlands along the Ariake Sea.

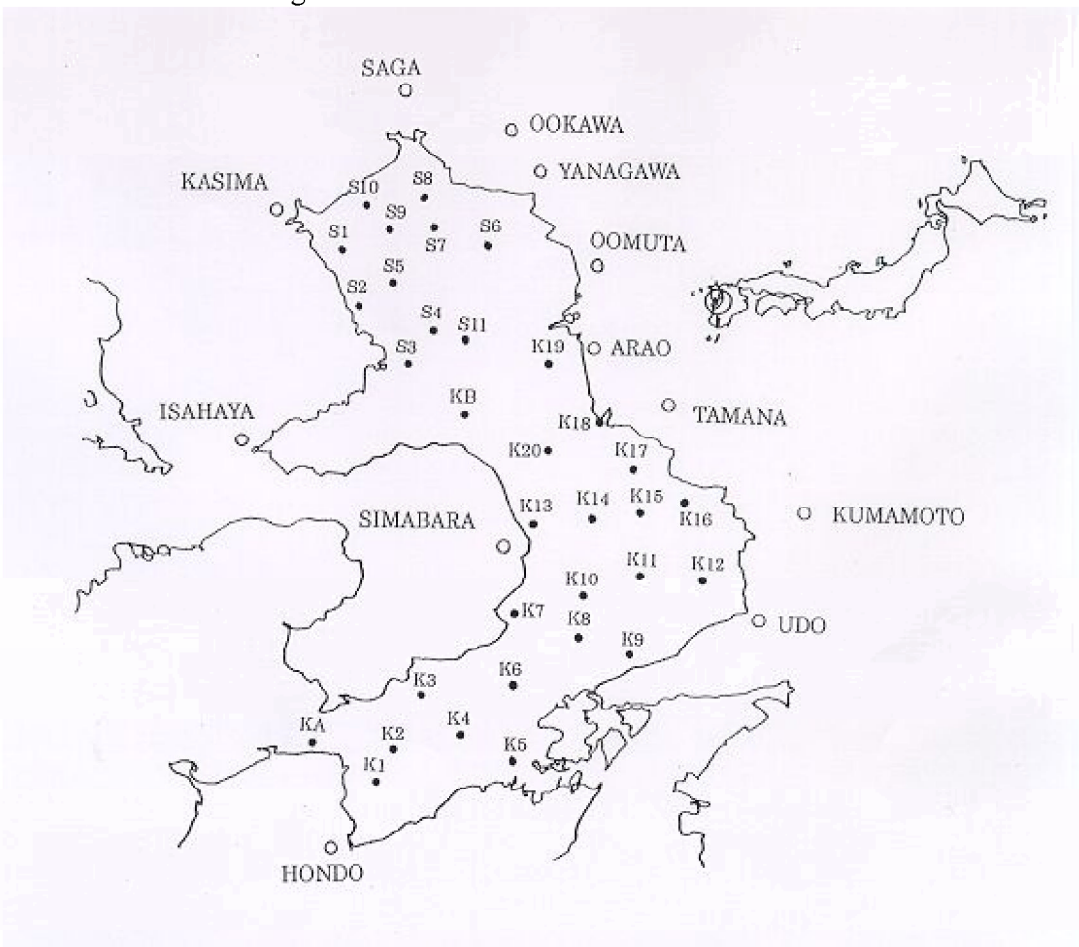


Fig. 1 A map of Ariake Sea and water quality sampling points

The mean annual temperature around the Ariake Sea is about 16 °C, the rainfall is about 2000 mm in the surrounding plain area and 2400 to 2800 mm in the mountainous area. The wind speed is about 2 to 2.5 m/sec and is most northward, northeasterly or westwards. The winter water temperature (January and February) is about 10 to 13 °C at the bay outlet and 8 to 10 °C at the innermost part. The former has a summer (July) temperature of about 26 °C while the latter 28-29 °C. At the innermost part almost all year round Secchi disk depth (SDD) is less than 2 m but at the bay outlet it is about 8 m except in July when heavy rainfall reduces its SDD to about 5 m.

With the post war development of Saga, Nagasaki and other prefectures, the Ariake Sea may become polluted with various materials, such as organics, nutrients and suspended solids. Especially, around the head bay water qualities are over the environmental standards, while all of the water quality parameters meet the standards in other areas. These phenomena may depend on water movement and discharge of pollutant loading from land area, however details have not clarified yet. There are reports that the Japanese bluefish and several other fish population have decreased in the Ariake Sea, though the cause of their decrease is not yet to be confirmed. Therefore, it is essential to monitor the environmental conditions of the Ariake Sea, to prevent water pollution by human activities.

Watanabe and Seguchi (1987) studied the tidal characteristics of the Ariake Sea with observed data. They used the Band 6 (IR channel) of Landsat TM data to study its flow regime, Band 2 (visible channel) to study the dispersion of fresh water from rivers and exchange of seawater fluxes, and correlated its turbidity to Band 4 of TM data (Watanabe and Seguchi, 1988; Seguchi and Watanabe, 1989). They found that Band 6 of TM data could be used to estimate the sea surface temperature of the Ariake Sea.

## RESEARCH OBJECTIVES

There are many water quality parameters that are measured every month in the Ariake Sea, of which two are selected for this study, namely the Secchi Disk Depth (SDD) and the Sea Surface Temperature (SST). The primary objective is to examine/establish empirical relationships for retrieving SDD and SST from atmospherically corrected reflectance of Landsat-TM images of the Ariake Sea, Japan. Using the above-established relationship, a preliminary assessment of the temporal change in SDD of the Ariake Sea was carried out.

## RESEARCH METHODOLOGY

The data used were six selected images of Landsat-TM data and field data of SDD and sea water temperature over 33 sites across the Ariake Sea (see Fig. 1) sampled on the same day as the satellite images. There were some missing values and so in a few instances data collected a day before (or after) was used in the analysis. Many Landsat-TM images taken over the Ariake Sea between early 1980s' and late 1990s' were screened and finally six images between 1984 and 1990 (see Table 1) were selected, on the basis that these are images taken during clear and mostly cloud free days, and field data are available on these days or a day before/after in some sampling points.

Table 1 Parameters of six Landsat-TM images selected for the study and the corresponding time of high tide at Ariake Sea.

| Date | Local time image acquired | Sun azimuth angle ($\phi$) ($^o$) | Solar zenith angle ($\theta$) ($^o$) | Time of high tide at suminoe, Ariake Sea | Range of Secchi Disk Depth SDD (m) | Range of sea surface temperature ($^o$C) |
|---|---|---|---|---|---|---|
| 1984/9/27 | 10:24AM | 139 | 42 | 11:00AM | 0.8 – 6.8 | 24.7 – 26.6 |
| 1988/4/15 | 10:23AM | 126 | 35 | 8:30AM | 0.8 – 11.2 | 13.5 – 16.8 |
| 1988/5/17 | 10:24AM | 113 | 28 | 10:00AM | 0.8 – 8.5 | 17.8 – 21.1 |
| 1988/11/9 | 10:24AM | 152 | 55 | 9:00AM | 0.3 – 7.2 | 16.9 – 21.4 |
| 1990/11/15 | 10:13AM | 149 | 57 | 8:00AM | 1.0 – 7.8 | 16.6 – 20.1 |
| 1995/5/5 | 10:01AM | 112 | 34 | 12:00AM | | 17.6 – 19.8 |

These images were first geometrically corrected and the averaged spectral radiance of 4 x 4 windows of 30 m resolution pixels centered over each of 33 sampling sites was extracted. This strategy of taking the average values of 4 x 4 windows is to filter out the satellite data noise, the site location errors, and the tidal effects as much as possible. Finally, the spectral values were atmospherically corrected using the Lowtran 7 atmospheric model and climate data, and then regressed against the field data collected from 33 sampling points. The climate data used in Lowtran 7 were wind speed, rainfall, air temperature, and visibility for Saga, Fukuoka, Nagasaki and Kumamoto Prefectures.

## SATELLITE DATA

A research shows that it is possible to quantitatively relate Landsat-TM and CZCS data of Nimbus 7 to water quality parameters such as turbidity (NTU:Nephleometric Turbidity Units) or clarity (SDD:Secchi Disk Depth), suspended solids, chlorophyll, and so on (Tassan, 1987). Theoretically, the intensity and/or amount of sea upwelling radiance from the sea surface, especially the visible channels of Landsat-TM (see Table 2), should depend on the amount of contaminants present in the sea because the presence of contaminants changes the backscattering characteristics of the seawater. Also, the thermal channel (band 6) of Landsat-TM data has been found to relate to sea surface temperature (e.g., H. Mizuo, et al., 1998).

To ensure an accurate matching between sub-windows of pixel values and their corresponding on-site sampling points, Landsat images acquired over the Ariake Sea were first geometrically corrected with respect to a vector file of the Ariake Sea coastline using the GCPWorks of PCI image analysis software. In the two-step procedure, the pixel coordinates were first transformed using second order polynomial equations and pixel values were then re-sampled by cubic convolution.

Table 2 Landsat-TM 5 radiance parameters (source: Duguay and Ledrew, 1991), the averaged, $L_T(\lambda)$, for the November 15, 1990 Landsat image and the atmospherically emitted plus path radiance, $L_R(\lambda) + L_A(\lambda)$, estimated by Lowtran 7.

| TM band | Wave length $\lambda$ ($\mu$m) | Gain ($A_1$) (W m$^{-2}$ Sr$^{-1}$ $\mu$m$^{-1}$ DC$^{-1}$) | Offset ($A_o$) (W m$^{-2}$ Sr$^{-1}$ $\mu$m$^{-1}$) | Averaged $L_T(\lambda)$11/15/1990 (W m$^{-2}$ Sr$^{-1}\mu$m$^{-1}$) | $L_R(\lambda) + L_A(\lambda)$ by Lowtran 7 11/15/1990 | 5/17/1988 |
|---|---|---|---|---|---|---|
| 1 | 0.45 - 0.52 | 0.602 | -1.500 | 42.047 | 20.58 | 30.21 |
| 2 | 0.52 - 0.60 | 1.175 | -2.805 | 27.246 | 11.70 | 17.67 |
| 3 | 0.63 - 0.69 | 0.806 | -1.194 | 16.085 | 5.83 | 9.04 |
| 4 | 0.76 - 0.90 | 0.814 | -1.500 | 7.265 | 2.03 | 3.30 |
| 5 | 1.55 - 1.75 | 0.108 | -0.370 | 0.267 | 0.065 | 0.094 |
| 6 | 10.5 - 12.5 | 0.056 | 1.238 | 7.893 | 7.05 | 7.53 |
| 7 | 2.08 - 2.35 | 0.057 | -0.150 | 0.012 | 0.0074 | 0.012 |

However, not all the radiance reaching the satellite sensor contains information about the Ariake Sea because the amount of radiance reaching the satellite sensor, $L_T(\lambda)$ at wavelength $\lambda$ comprises essentially of three components: the sea surface radiance, $L_W(\lambda)$ which contains information about the water constituents; the atmospherically scattered radiance due to air particles (Rayleigh scattering), $L_R(\lambda)$ and the particulate or aerosol scattered radiance, $L_A(\lambda)$ (Aranuvachapun and LeBlond, 1984).

$$L_T(\lambda) = L_W(\lambda) + L_R(\lambda) + L_A(\lambda) \quad (1)$$

For studies involving multi-date images, atmospheric correction is essential because water quality variables are related to $L_W(\lambda)$, not $L_T(\lambda)$, and $(L_R(\lambda) + L_A(\lambda))$ changes with the atmospheric conditions which vary from image to image. Many approaches have been attempted to estimate $L_R(\lambda)$ and $L_A(\lambda)$ (e.g., Caselles and Garcia, 1989; Richter, 1991). One of the simplest approaches is to determine the dark pixel characteristics of the site of interest and subtract it from $L_T(\lambda)$ as atmospheric correction (Pattiaratchi et al. 1994). More sophisticated methods are such as the temporal change detection technique based on image differencing, image ratioing, image regression plus a threshold, and multistage decision logic using a decision tree (Singh, 1989).

In this study, the Lowtran 7 atmospheric model of Knetzys et al. (1989) was used to estimate $(L_R(\lambda) + L_A(\lambda))$. Table 2 shows the values of $L_R(\lambda)$ and $L_A(\lambda)$ estimated through Lowtran 7 for November 15, 1990 and May 17, 1988 over the Ariake Sea based on atmospheric data for the mid-latitude climate and navy maritime aerosol. Lowtran 7 computes all the thermal radiation emitted by the atmosphere (called atmosphere radiance in Lowtran 7) and all the solar radiation scattered by the atmosphere (called path radiance). The former has been found to be negligible for wavelengths in the visible, near infrared (near IR) and infrared (IR) range (0.45 to 2.35 μm) but the latter can be as high as 30 $Wm^{-2}Sr^{-1}\mu m^{-1}$ (see Table 2). The total radiation reaching the Landsat-TM sensor is highest at Channel 1 (0.45–0.52 μm), but it generally does not exceed beyond 50 $Wm^{-2}Sr^{-1}\mu m^{-1}$ at Channel 1 for the 6 images acquired over the Ariake Sea. Essentially this means that out of the total radiance received by the Landsat-TM sensor, only about 40 to 50% contains information of the Ariake Sea. According to Hovis and Leung (1977) and Austin (1974), the percentage of the total radiance received by the Landsat-TM sensor that contains information of the oceanic surface could be as little as 30%.

## WATER QUALITY DATA

Since tidal effects could affect both the accuracy of water quality and satellite data sampled from the sea, the water level change of the Ariake Sea was checked at Suminoe during the days the Landsat-TM images were taken. Most Landsat-TM images were acquired at about 10:00 A.M. It would be ideal if the high and low tide of the Ariake Sea on that day also occurs around the same time (10:00 A.M.) because the magnitude of water velocity will be very small when high and low tide occurs. It would also be ideal to collect all field data around 10:00 A.M. but this was not possible in view of the size of Ariake Sea. From Table 1, it seems that the data on 9/27/1984, 5/17/1988 and 11/9/1988 should be least affected by the tide. The data on 11/15/1990 and 4/15/1998 could be slightly affected by the tides.

### Secchi Disk Depth

Nephleometric Turbidity Units (NTU) is the commonly used measurement for turbidity, which is the degree of opaqueness, or transparency produced in water by suspended particulate matters. Turbidity changes with the balance of influx and outflux of a water body and the amount of contaminants present in the water. A number of studies have been conducted on estimating the turbidity of large lakes, sea and estuaries using Landsat-TM data, e.g., Abiodun (1976), Abiodun and Adeniji (1978), Khorram (1985). Carpenter and Carpenter (1983) used Landsat data to study the turbidity for inland lakes in southeastern Australia. Ritchie et al. (1984) used TM bands 1, 2, 3 and 4 to relate reflectance with sediment concentration of Lake Chicot, Arkansas. Pattiaratchi et al. (1994) and Thomas (1980)

monitored the temporal changes of coastal turbidity and tidal cycles with multi-temporal Landsat images.

In this study, instead of turbidity, the Secchi disk depth (SDD) (Reid, 1965) is used, which is a measure of water clarity or the light attenuation due to suspended sediment and organic materials present in the sea water. Even though somewhat subjective, SDD is a practical way to measure the turbidity of water. The SDD measurement involves dipping a 20 cm diameter white disk into the water and measuring the averaged depths when the disk disappears, and appears again when it is drawn back. Essentially, the disk disappears at a depth where the amount of sunlight transmitted is approximately 5%. Therefore, theoretically the amount of radiance that the satellite sensor receives should be inversely related to the Secchi depth measurements, and it should be possible to develop empirical relationships between them (e.g., Pattiaratchi et al., 1994; Bagheri and Dios, 1990). The correlation coefficients in Table 3 show that visible channels of Landsat-TM data are inversely correlated to SDD, but the degree of correlation has been found to vary from image to image mainly because of data noise and measurement errors.

Table 3 The correlation coefficients of $L_w(\lambda)$ retrieved from Landsat-TM images versus SDD, and $L_w(\lambda)$ versus SST for Ariake Sea

| TM band | Correlation, $L_w(\lambda)$ vs. SDD 5/7/1988 image | Correlation, $L_w(\lambda)$ vs. SDD 11/15/1990 image | Correlation, $L_w(\lambda)$ vs. SST 11/15/1990 image |
|---|---|---|---|
| 1 | -0.794 | -0.437 | -0.379 |
| 2 | -0.846 | -0.560 | -0.522 |
| 3 | -0.799 | -0.493 | -0.502 |
| 4 | -0.548 | -0.249 | -0.302 |
| 5 | -0.522 | -0.131 | -0.217 |
| 6 | - | 0.458 | 0.649 |
| 7 | -0.497 | -0.095 | -0.185 |

### Sea Surface Temperature

Sea surface temperature (SST) exerts a major influence on our climate and is under close monitoring by climatologists throughout the world. Lately, SST at global scale has been mapped out on a regular basis using the thermal channel of NOAA-AVHRR data. From an environmental perspective, SST of water bodies like lakes or inland sea could go beyond a stage where marine life is threatened, either directly or indirectly. It is called thermal pollution, which could happen from effluent discharged by factories and thermal electric plants.

## REGRESSION ANALYSIS

### Empirical Relationships

The empirical relationships developed in this study are site-specific because environmental conditions vary from place to place. Furthermore, these empirical relationships could change with time because the types of constituents in the water will likely not remain constant; neither will the atmospheric composition over the Ariake Sea. However, these relationships are established assuming that basic environmental conditions remain unchanged, e.g., constant atmospheric emissivities in the 0.45 to 12.5 μm range. There are theoretical models developed relating soil moisture (e.g., Biftu and Gan, 1999) to radiation, e.g., radiative

transfer model, but to the knowledge of the authors, there is not yet a theoretical model developed that relate the turbidity of seawater to radiation. Furthermore, the lack of adequate data makes theoretical models applicable only under a carefully controlled research environment.

Linear Regression

From the magnitudes of $L_T$, $L_R$ and $L_A$ listed in Table 2, it is clear that in terms of magnitude, channels 1 to 3 should exert considerably larger influence over the model results than that of channels 4 to 7 whose values could be several orders smaller. Many algorithms have been examined but only nine different forms of linear regression equations are herein presented.

$$SDD = k + \alpha_1 TM_1 + \alpha_2 TM_2 + \alpha_3 TM_3 \quad (2)$$
$$SDD = \alpha_1 TM_1 + \alpha_2 TM_2 + \alpha_3 TM_3 \quad (3)$$
$$\log(SDD) = k + \alpha_1 TM_1 + \alpha_2 TM_2 + \alpha_3 TM_3 \quad (4)$$
$$\log(SDD) = \alpha_1 TM_1 + \alpha_2 TM_2 + \alpha_3 TM_3 \quad (5)$$
$$\sqrt{SDD} = k + \alpha_1 TM_1 + \alpha_2 TM_2 + \alpha_3 TM_3 \quad (6)$$
$$\sqrt{SDD} = \alpha_1 TM_1 + \alpha_2 TM_2 + \alpha_3 TM_3 \quad (7)$$
$$\sqrt{SDD} = \alpha_1 TM_1 + \alpha_2 TM_2 + \alpha_3 TM_3 + \alpha_4 (TM_1)(TM_2) \quad (8)$$
$$SDD = k + \alpha_1 TM_1 + \alpha_2 TM_2 + \alpha_3 TM_3 + \alpha_4 TM_4 + \alpha_5 TM_5 + \alpha_6 TM_7 \quad (9)$$
$$SDD = \alpha_1 TM_1 + \alpha_2 TM_2 + \alpha_3 TM_3 + \alpha_4 TM_4 + \alpha_5 TM_5 + \alpha_6 TM_7 \quad (10)$$

These algorithms, representing different levels of complexities, assume that SDD is related to the linearly weighted sum of responses from various visible, near IR and IR wavelengths of the Landsat-TM sensor. Equations (3), (5) and (7) are attempted because they assume that the independent variables fully explain the variance of the dependent variable, e.g., SDD. Conversely, the k-intercept represents the unexplained variance of the independent variables. Albeit such an assumption is rarely true, Eqs. (3), (5) and (7) are included for the purpose of comparing with their counterparts with the k intercept.

Table 4 Calibrated parameters of linear regressive models (Eqs. 2 to 10) between Secchi Disk Depth (SDD) and reflectance of Landsat-TM ($L_w(\lambda)$) images for Test case 3

| Equat -ion | (2) | (3) | (4) | (5) | (6) | (7) | (8) | (9) | (10) |
|---|---|---|---|---|---|---|---|---|---|
| $k$ | 4.1279 | | 0.8751 | | 1.8041 | | | 4.6491 | |
| $\alpha_1$ | 0.5048 | 0.6839 | 0.1858 | 0.2238 | 0.1472 | 0.2254 | 0.2090 | 0.2525 | 0.5143 |
| $\alpha_2$ | -0.9844 | -0.8731 | -0.3068 | -0.2833 | -0.2652 | -0.2165 | -0.2077 | -0.6769 | -0.6085 |
| $\alpha_3$ | 0.4575 | 0.1563 | 0.1023 | 0.0385 | 0.1076 | -0.0241 | 0.1146 | 0.0675 | -0.2157 |
| $\alpha_4$ | | | | | | | -0.0021 | 0.7943 | 0.5964 |
| $\alpha_5$ | | | | | | | | 1.8102 | 1.3558 |
| $\alpha_6$ | | | | | | | | -12.455 | -8.3822 |

Table 3 shows that for the data on 11/15/1990, SDD are more negatively correlated to channels 1 to 3 of Landsat-TM than channels 4 to 7. These inverse relationships make sense because seawater of higher SDD values (which means larger clarity or smaller opacity) should generally reflect less radiation into the atmosphere. Given that channels 1 to 3 are more strongly correlated to SDD, Eqs. (2) and (3) were tested, that are simple linear regressions

(respectively with and without the intercept parameter $k$) between SDD and the three visible channels, $TM_1$, $TM_2$, and $TM_3$ of Landsat-TM. $TM_1$ corresponds to $L_W(\lambda)$ of Eq. (1) where $\lambda$ ranges from 0.45 to 0.52 μm, and so on (see Table 2).

Equations (4) to (8) are the simple extensions to Eqs. (2) and (3) such that SDD is log transformed in Eqs. (4) and (5) and square rooted in Eqs. (6) to (8). Therefore strictly speaking, Eqs. (4) to (8) are nonlinear. For example, Eq. (4) can be re-written as SDD = exp ($k + \alpha_1 TM_1 + \alpha_2 TM_2 + \alpha_3 TM_3$). The idea of testing Eqs. (4) to (8) is to examine whether SDD is more than linearly related to the Landsat-TM data, as postulated by researchers such as Aranuvachapun and LeBlond (1981), Carpenter and Carpenter (1983), and Khorram (1985). Equations (9) and (10) are tested to check whether SDD is also related to the near IR and IR channels of Landsat-TM. Even though theoretically SDD should be primarily linked to the visible channel, the above researchers and others also found relationships between water quality variables like turbidity, suspended solids, etc. with the near IR or IR channels of Landsat-TM or Landsat-MSS.

Using the linear regression modules of a commercial statistical software called SPLUS, the parameters for the above algorithms, namely $k$, $\alpha_1$ to $\alpha_6$, were derived through calibrating the algorithms with respect to in-situ SDD measurements, single and multi-date Landsat-TM data (see Table 4). To ensure that the model parameters obtained are conceptually realistic, the calibrated algorithms are validated with data sets independent of their calibration experience. Quite a number of retrieval algorithms published in the literature have not been validated.

Table 5 Correlation coefficient (ρ) and bias (%) of 4 cases of linear regressive models (Eqs. (2) to (10)) at both calibration and validation stages between Secchi Disk Depth (SDD) and reflectance of Landsat-TM ($L_w(\lambda)$) images (Atmospherically and Geometrically Corrected) for Ariake Sea, Japan.

| Case | Dates of Landsat-TM images | Mode | | Eq. (2) | Eq. (3) | Eq. (4) | Eq. (5) | Eq. (6) | Eq. (7) | Eq. (8) | Eq. (9) | Eq. (10) |
|---|---|---|---|---|---|---|---|---|---|---|---|---|
| 1 | 4/15/1988 | C | ρ | 0.84 | 0.84 | 0.85 | 0.84 | 0.85 | 0.85 | 0.85 | 0.89 | 0.88 |
| | | | Bias | 0 | 0.07 | -5.69 | -5.46 | -2.98 | -3.03 | -3.01 | 0 | 0.10 |
| | 5/17/1988 | V | ρ | 0.53 | 0.57 | 0.83 | 0.79 | 0.77 | 0.69 | 0.54 | 0.58 | 0.58 |
| | | | Bias | 84.4 | 63.6 | -15.6 | 36.3 | 36.9 | 94.3 | 140.2 | 161.7 | 129.2 |
| | 11/15/1990 | V | ρ | 0.02 | 0.06 | 0.10 | -0.01 | 0.05 | -0.02 | -0.01 | -0.20 | -0.19 |
| | | | Bias | -1.44 | 5.59 | 7.90 | 6.90 | 0.72 | -13.4 | -16.3 | 53.4 | 64.7 |
| 2 | 4/15/1988 + 5/17/1988 | C | ρ | 0.79 | 0.74 | 0.70 | 0.49 | 0.78 | 0.58 | 0.77 | 0.86 | 0.78 |
| | | | Bias% | 0 | -3.29 | -6.88 | -7.21 | -3.93 | -6.69 | -3.98 | 0.0 | -3.91 |
| | 11/15/1990 | V | ρ | 0.60 | 0.63 | 0.63 | 0.60 | 0.61 | 0.49 | -.10 | 0.21 | 0.46 |
| | | | Bias% | 23.4 | -17.1 | 0.58 | -31.2 | 12.5 | -46.7 | -6.05 | 65.5 | 6.47 |
| 3 | 4/15/1988 + 5/17/1988 + 9/27/1984 + 11/9/1988 | C | ρ | 0.75 | 0.72 | 0.68 | 0.55 | 0.77 | 0.59 | 0.74 | 0.80 | 0.74 |
| | | | Bias | -9.0 | -2.9 | 8.18 | 8.50 | 4.25 | 6.50 | 4.56 | 0.0 | -3.1 |
| | 11/15/1990 | V | ρ | 0.80 | 0.67 | 0.79 | 0.66 | 0.80 | 0.50 | 0.23 | 0.58 | 0.63 |
| | | | Bias | 13.9 | -24.4 | -11.8 | -35.4 | 1.75 | -52.8 | -24.5 | 16.4 | -26.5 |
| 4 | 9/27/1984+ 11/9/1988 | C | ρ | 0.78 | 0.73 | 0.79 | 0.70 | 0.81 | 0.64 | 0.80 | 0.80 | 0.74 |
| | | | Bias | 0.0 | -2.2 | -8.0 | -8.7 | -3.7 | -5.6 | -3.8 | 0 | -2.2 |
| | 5/17/1988 | V | ρ | 0.77 | 0.70 | 0.92 | 0.91 | 0.93 | 0.84 | 0.93 | 0.80 | 0.74 |
| | | | Bias | -40.9 | -19.2 | -40.3 | -33.9 | -40.1 | -19.5 | -39.1 | -48.7 | -21.3 |
| | 11/15/1990 | V | ρ | 0.78 | 0.70 | 0.83 | 0.70 | 0.81 | 0.52 | 0.54 | 0.50 | 0.54 |
| | | | Bias | 13.1 | -33.6 | 8.78 | -36.8 | 11.9 | -58.9 | -29.0 | 9.44 | -36.6 |
| | 4/15/1988 | V | ρ | 0.80 | 0.80 | 0.84 | 0.83 | 0.85 | 0.84 | 0.98 | 0.79 | 0.79 |
| | | | Bias | 1.7 | -26.7 | 18.4 | -19.9 | 7.49 | -41.1 | -14.5 | 0.56 | -27.4 |

## DISCUSSIONS OF RESULTS

Statistical indices selected to compare the performance of the retrieval algorithms are bias (Bias), the coefficient of determination ($R^2$), or correlation coefficient ρ. The retrieval algorithms are assessed according to the calibration and validation results (in terms of $R^2$ and Bias) of test cases 1 to 4 for the linear regression models (see Table 5). Comparisons between predicted variables (SDD or SST) and in-situ measurements are done in terms of the above statistics and scatterplots (see Fig. 2).

The accuracy of SDD retrieved from Landsat-TM data would primarily depend on the adequacy of the retrieval algorithm and the data used in model calibration and validation. At first, the data and the calibration exercise will be discussed in the followings.

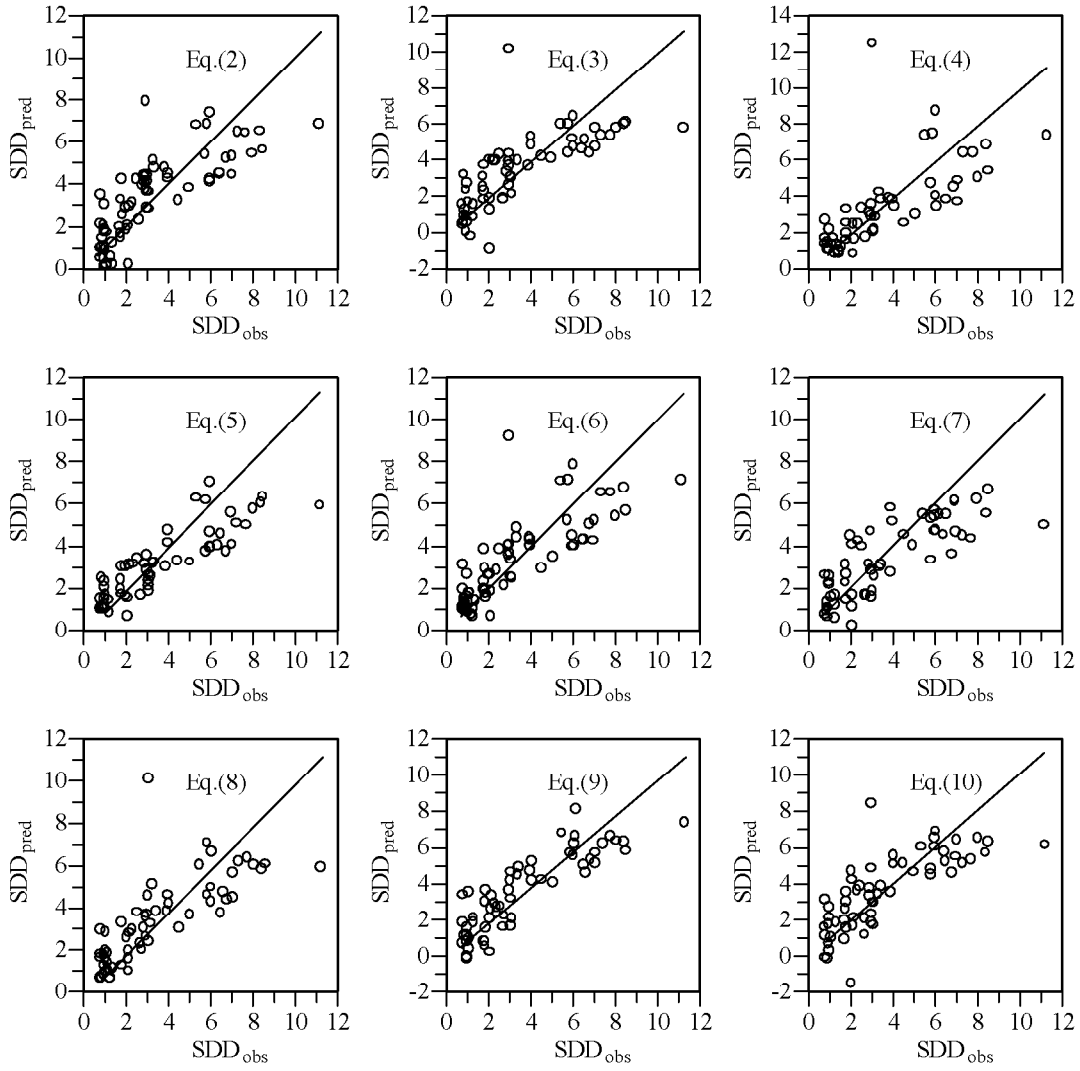


Fig. 2 Scatterplots of predicted versus observed Secchi disk depth of Ariake Sea for both the calibration and validation stages of linear regressions using Test Case 3 data, calibration

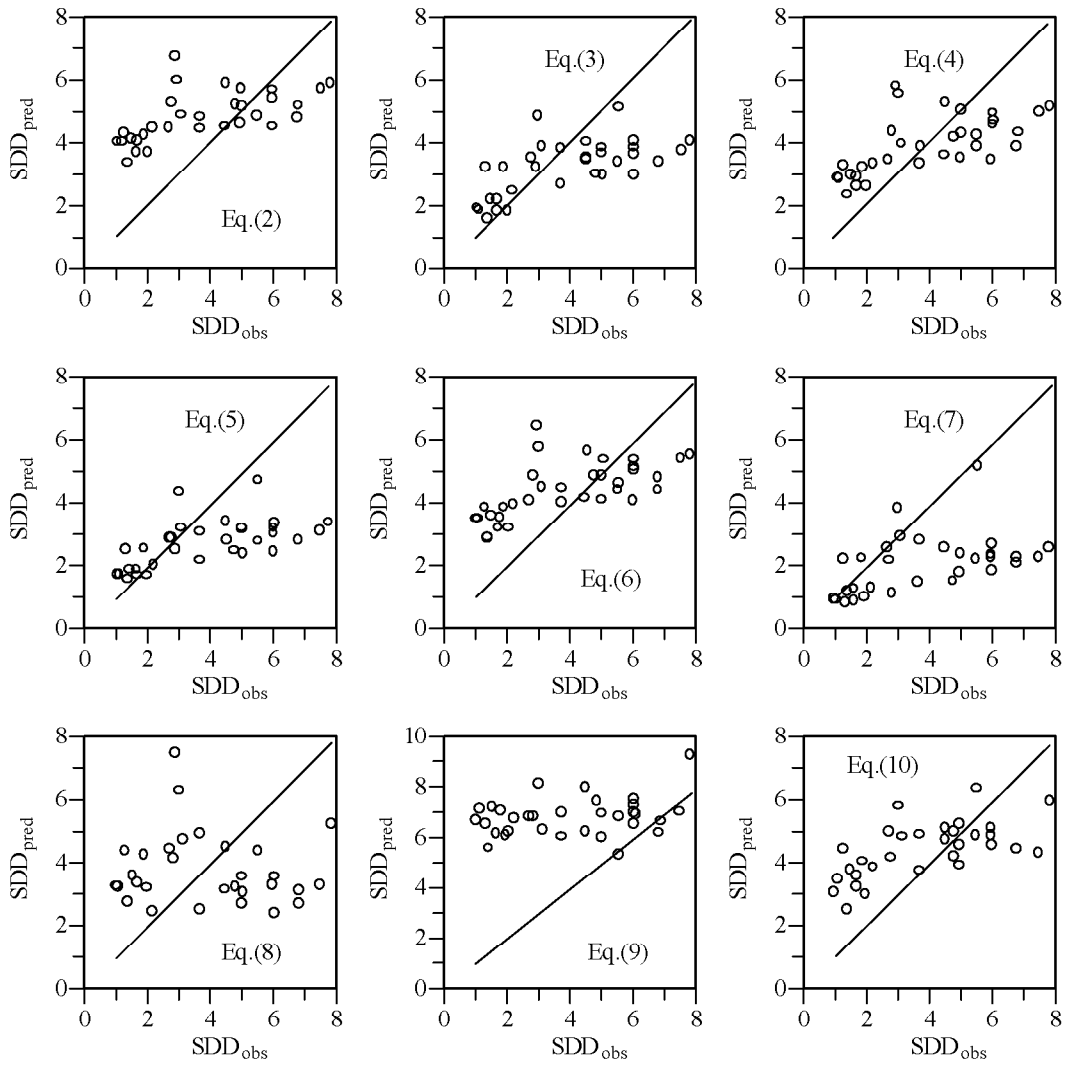


Fig. 2 (continued): Scatterplots of predicted versus observed Secchi disk depth of Ariake Sea for both the calibration and validation stages of linear regressions using Test Case 3 data, validation

Calibrated model parameters depend on the calibration data because by adjusting the parameters until the difference between the simulated and observed SDD is minimized. The final parameters are inevitably related to the calibration data. A sufficient and good quality data set is always essential to achieve a good calibration and to activate all the model parameters during the calibration stage. Because complications from non-representative data, measurement errors, data noise and model structure often prevent us from developing meaningful retrieval algorithms, irrespective of what model it is.

Since the actual atmospheric radiosonde data over the Ariake Sea at the time satellite images were taken is not available, Lowtran 7 was operated using the standard atmospheric data provided in the software and so a certain amount of error is expected in the estimated $L_R(\lambda) + L_A(\lambda)$. Furthermore, SDDs are point measurements which contain measurement errors,

while atmospherically corrected Landsat-TM spectral values are spatially averaged data with data noise resulted from the heterogeneous characteristics of sea surface, atmospheric circulation and other related factors. At 30 m resolutions, a 4 x 4 window of Landsat data represents a sea surface 120 x 120 m in size. The combined effects of non-representative data, measurement errors, data noise, and model structure further complicate the data dependency feature of model calibration. Essentially, the calibration exercise that involves matching point data (SDD) with spatial measurements ($L_W(\lambda)$) will not result in "error-free" or completely realistic parameters.

Therefore albeit it is impossible to obtain a unique set of parameters, in many instances it should be possible to obtain a set of parameters that are conceptually realistic. A parameter set that is not realistic conceptually will likely perform poorly when operating under forecast or prediction modes. The validation stage is designed to assess if a set of parameters is conceptually sound. Decrease in model performances would be expected when the calibrated model is applied to the validation stage, but the decrease should be fairly modest. A drastic decrease in model performances at the validation stage could mean either one or more of the following problems: (a) the retrieval algorithm does not have adequate model structure or are not physically sound, (b) its calibrated parameters are conceptually unrealistic, and (c) the calibration and/or validation data are non-representative because of measurement errors.

Even though not always the case, a larger data set usually contains a wider range of information than a small data set, if both data sets are of similar quality. In this regard, the use of multi-date Landsat-TM images usually has the advantage over single date Landsat image. In other words, the data dependency feature of almost any retrieval algorithm means that using data, which encompass a wide range of information, would have a better chance of achieving meaningful calibration or realistic calibrated parameters. This is evident from Table 5 where the validation result on 11/15/1990 of Case 3 (which used four sets of calibration data) is better than that of Case 2 (which used two sets of calibration data) which in turn is better than that of Case 1 (which only used one set of calibration data).

Secchi Disk Depth (SDD)

Case 1 is based on one set (4/15/1988) while Case 2 is based on two sets (4/15/1988 + 5/17/1988) of calibration data (see Table 5). In terms of $R^2$ and Bias, Case 1 was slightly better than Case 2 at the calibration stage. However, based on the validation data on 11/15/1990, Case 2 performed much better than Case 1. For Case 2, the first six equations have $\rho$ values of about 0.60 but Case 1 has correlation coefficient ($\rho$) ranging from –0.20 to 0.10. Case 2 did better than Case 1 probably because using two data sets should generally lead to more dependable or realistic calibration than one data set because the former likely contain a wider range of information.

For Case 1, its validation result based on the 5/17/1988 data set shows relatively better $\rho$ (0.53 to 0.83) but the bias can also be high (e.g., over 160% for Eq. (9)). This could be because both 4/15/1988 and 5/17/1988 data sets have relatively similar atmospheric conditions (both were of spring season and separated by a month), as reflected by relatively high $\rho$ obtained for the validation stage using the 5/17/1998 data. However, bias is high and positive partly because the average SDD of the calibration data (3.6 m) dated 4/15/1988 was higher than that of the validation data (3.34 m) dated 5/17/1988. Besides that, there could be other problems with the calibration because the overall bias for the 11/15/1990 validation is still positive even though the average SDD (3.95 m) for 11/15/1990 is higher than that of 4/15/1988. It could be partly because linear regressions do not accurately represent the relationship between SDD and the spectral values of Landsat-TM.

It seems that Case 2 performs better than Case 1 mainly because the former used more calibration data. In order to confirm this, Case 3 was conducted, that involved four data sets mixed between spring and autumn data (Table 5). At the calibration stage, between Case 1 to Case 3, the performance of Case 1 would rank first, then Case 2 and finally Case 3 but their differences are fairly marginal. However at the validation stage, the performance ranking becomes reversed and the differences are substantial, especially between Case 1 and Case 2, e.g., Case 1 is much poorer than Case 2. Again, Case 3 outperformed the other two cases probably because its calibration data encompasses a wider range of information.

Besides the calibration data, it seems that the result also depends on the type of regression model used. Between Eqs. (2) and (10), Eqs. (2) to (6) generally performed better than Eqs. (7) to (10). This probably shows that SDD is primarily related to the spectral reflectance of the visible channels, 1 to 3, than the near IR or IR channels, 4 to 7, or the addition of the latter channels "complicate" the SDD/spectral reflectance relationship. This speculation is also partly backed up by the correlation matrix between the TM bands of 11/15/1990 image and SDD. Table 3 shows that the first three channels are more negatively correlated to SDD than 4,5 or 7. Furthermore, there seems no clear advantage in transforming SDD to logarithmic space or square root, and more complicated regression models (e.g., Eq. (8) that involve interactions between Channels 1 and 2) could end up in worse validation results.

Cases 1 and 2 used spring calibration data while Case 3 used a mixture of spring and autumn data. The idea behind Case 4 is to reverse the test strategy by using autumn calibration data (9/27/1984 and 11/9/1988) with spring and autumn validation data. Virtually all three sets of validation results are satisfactory (relatively high ρ) but the Bias could be as high as about –60%. There is more negative bias than positive and this could be partly explained in terms of the average SDD because the average SDD (9/27/1984 + 11/9/1988) of 3.28 m is less than that of the validation data (3.34 m to 3.95 m). However, part of the bias could also be caused by the use of linear regression models because between Eqs. (2) to (10), the bias could range from +13.1% to –58.9%, even though they were all tested with the 11/15/1990 data.

A perusal of Table 4 shows that there is no extremely large or small value and so generally calibrated parameters are deemed reasonable. Therefore linear regression itself may not be the most appropriate retrieval algorithm(s) for converting Landsat-TM spectral values to SDD. From optical physics, it is known that the atmospherically and geometrically corrected reflectance $L_w(\lambda)$ (or $TM_1$ to $TM_7$) at visible wavelengths (also possibly near IR and IR) should be related to the optical properties of seawater, which in turn is related to its opacity/clarity, e.g., SDD (see Table 3). Therefore these regression models should contain some essential elements of transforming seawater clarity (SDD) to spectral reflectance received by the Landsat-TM sensor. However, the simple, input/output model structure of these linear models also mean that they are simplified versions of nature, and they ignore certain interactive or stand alone factors of the atmosphere and the water body that contribute to the measured $Lw(\lambda)$ and SDD. This conjecture will be tested with nonlinear regression and neural network models in future research.

Finally, the "best" linear regression model of Case 3 is used to map the SDD of Ariake Sea. Plate 1 shows the SDD map of Ariake Sea estimated from Landsat-TM data dated May 17, 1988 using Eq. (6) calibrated with Test Case 3 data. Plate 2 shows the SDD map corresponding to a Landsat-TM imaged dated May 5, 1995. Between these two maps, it seems that the Ariake Sea had higher clarity in May 5, 1995 than in May 17, 1988. However, there is little basis to judge the temporal change of SDD for the Ariake Sea from these two maps. More SDD maps estimated from multi-year Landsat-TM images should be carried out before considering the temporal change of the water clarity of Ariake Sea.

Sea Surface Temperature (SST)

It has been demonstrated theoretically (Price, 1983) and experimentally (Gibbons et al. 1989; Seguchi and Watanabe, 1989; Pattiaratchi et al., 1991) that sea surface temperature (SST) can be accurately retrieved from thermal infrared data, such as the channel 6 of Landsat-TM (Table 1). Pattiaratchi et al. (1994) even conjectured that SST might be retrievable from channel 3 of Landsat-TM because watercolor and temperature are indirectly correlated. During the experiments of Case 3 on SST of the Ariake Sea, it was possible to obtain good linear and nonlinear regressive relationships between SST and channels 1, 2, 3, 4, 5, and 7 of Landsat-TM at the calibration stage. However, the results at the validation stage, such as those conducted for SDD, are generally very poor, which indicate that good calibration results only reflect good curve-fitting but it has little physical basis.

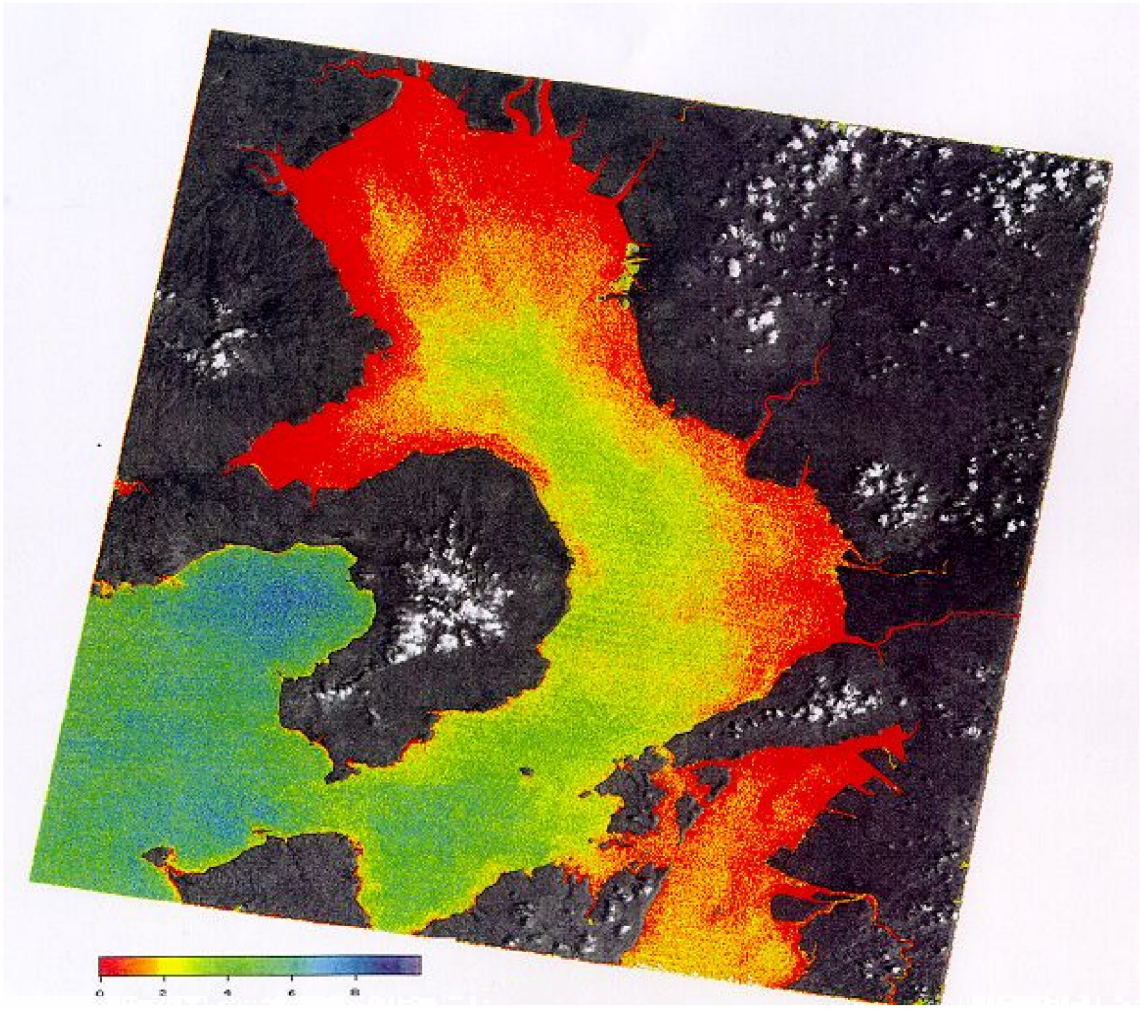

Plate 1 A Secchi Disk Depth (SDD) map of Ariake Sea estimated from the Landsat-TM image dated May 17, 1988 using Eq. (6) calibrated with Test Case 3 data

Among the six selected Landsat-TM images, only three images (9/27/1984, 11/15/1990 and 5/5/1995) have valid reflectance values for channel 6. Then atmospherically corrected radiance, $L_W(\lambda_6)$ or $TM_6$ of these 3 images are regressed against SST collected over the same

33 sampling points of the Ariake Sea (Table 6). Since only channel 6 data is involved, only a simple linear regression algorithm is necessary, e.g.,

$$SST = k + \alpha_1 TM_6 \tag{11}$$

From applying a single date data to a simple linear regression Eq. 11 for test Cases 5 and 6, the calibration and validation results obtained in terms of ρ (Table 6) merely reflect the correlation (ρ) between $L_W(\lambda_6)$ and SST, which is 0.30 for the 9/27/1984 data and 0.65 for the 11/15/1990 data. The result is fairly modest partly because it basically reflects the correlation between $L_W(\lambda_6)$ or $TM_6$ and SST. It can vary quite significantly from image to image because of measurement errors of ground data, data noise of satellite data and the tidal effects on SST, since it is not possible to collect all ground data at the instance the satellite image was taken. Furthermore, it is noted that the resolution of Channel 6 of TM is only about 120 m. However, the results indicate a potential of predicting SST from the thermal channel of Landsat-TM data, as found by other researchers.

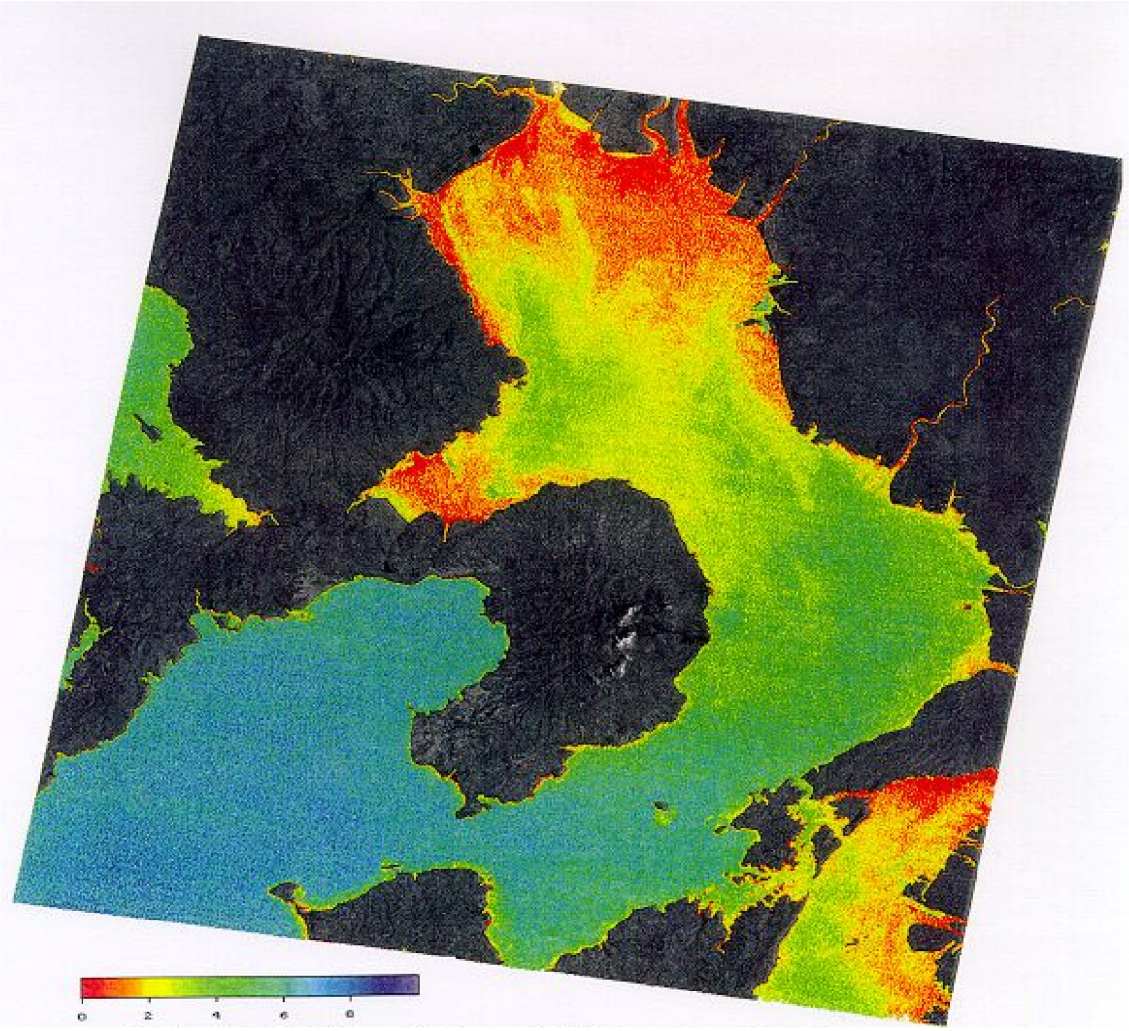

Plate 2 A Secchi Disk Depth (SDD) map of Ariake Sea estimated from the Landsat-TM image dated May 5, 1995 using Eq. (6) calibrated with Test Case 3 data

Table 6 Correlation coefficient (ρ) and bias (%) of simple regressive models (Eqs. (11) to (12)) at both calibration and validation stages between Sea Surface Temperature (SST) and channel 6 reflectance of Landsat-TM ($L_w(\lambda_6)$) images (Atmospherically and Geometrically Corrected) for Ariake Sea, Japan.

| Case | Dates of Landsat-TM images | Mode | ρ | Bias (%) | Equation |
|---|---|---|---|---|---|
| 5 | 11/15/1990 | C | 0.65 | 0.00 | 11 |
| | 9/27/1984 | V | 0.30 | -8.19 | |
| 6 | 9/27/1984 | C | 0.30 | 0.00 | 11 |
| | 11/15/1990 | V | 0.65 | 11.74 | |
| 7 | 9/27/1984+ 5/5/1995 | C | 0.78 | 0.00 | 11 |
| | 11/15/1990 | V | -0.41 | -2.1 | |
| 7 | 9/27/1984+ 5/5/1995 | C | 0.99 | 0.00 | 12 |
| | 11/15/1990 | V | 0.41 | 0.00 | |

To employ multi-date calibration data for SST, given that SST varies significantly from season to season (see Table 1), e.g., mean SST for 9/27/1984 data was 18.86 °C while that for 11/15/1990 data was 25.24 °C, it is probably better to de-center SST or to remove the sample mean ($\mu_{SST}$) from SST before doing the regression, e.g.,

$$(SST - \mu_{SST}) = k + \alpha_1(TM_6 - \mu_{TM6}) \tag{12}$$

Also, to be consistent, the channel 6 data is also de-centered. In this case, both the dependent and independent variables have zero mean. This conjecture is proved useful in test Case 7 that involves two sets of calibration data (9/27/1984 + 11/15/1990). Better result (both calibration and validation) is obtained from Eq. (12) than Eq. (11) because the former uses de-centered data. Plate 3 shows the SST map of Ariake Sea estimated from the Landsat-TM image dated 11/15, 1990 using Eq. (18) calibrated with Case 7 data.

Lastly, SST can also be derived from Landsat-TM data using Schott and Volchok (1985) equation as:

$$T_s = \frac{k_2}{\ln(k_1 / L(\lambda) + 1)} \tag{13}$$

Where $k_1$ is a first constant (66.776 mW cm$^{-2}$ Sr$^{-1}$ μm$^{-1}$ for TM-6), $k_2$ is a second constant (1260.56 $^{o}K$ for TM-5), and $L(\lambda)$ is the radiance derived from Landsat TM band 6 digital numbers (mW cm$^{-2}$ Sr$^{-1}$ μm$^{-1}$). $T_s$ represents the amount of radiation thermally emitted by an object, which is related to the physical temperature of the object and its dielectric property. However, a preliminary estimate of SST using LandsatTM data and Eq. (13) shows little correlation with the observed data.

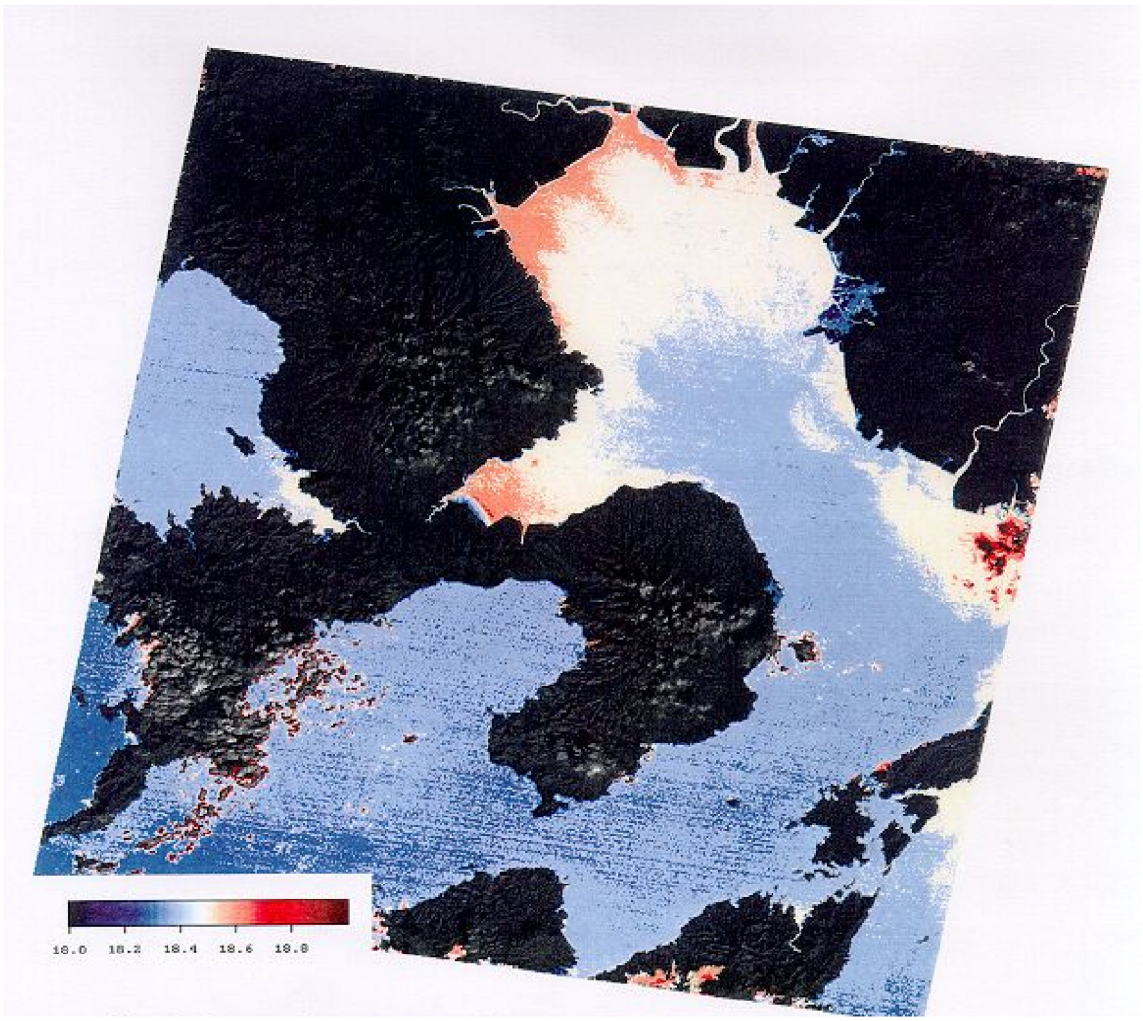


Plate 3 A Sea Surface Temperature (SST) map of Ariake Sea estimated from the Landsat-TM image dated November 15, 1990 using Eq. (12) calibrated with Case 7 data

## SUMMARY AND CONCLUSIONS

Through the estimation of Rayleigh scattering ($L_R(\lambda)$) and the particulate or aerosol scattered radiance ($L_A(\lambda)$) in Lowtran 7, the radiance reflected at the sea surface ($L_W(\lambda)$) is derived from the measured radiance, $L_T(\lambda)$, of geometrically corrected Landsat-TM images taken over the Ariake Sea. Then $L_W(\lambda)$ averaged from 4 x 4 windows of pixels centered at 33 sampling sites was regressed against the observed Secchi Disk Depth (SDD) using linear regression algorithms.

Results show that using multi-date, visible channels of Landsat-TM as the calibration data predict more accurate and dependable SDD at the validation stage than using single-date, calibration data of Landsat-TM. This study confirms the feasibility of retrieving SDD (or turbidity/ suspended sediments as shown by other researchers) from Landsat-TM data. Preliminary analysis using limited data shows that the Ariake Sea had higher clarity in May 5, 1995 than in May 17, 1988. However, we cannot adequately consider the temporal change of water clarity in the Ariake Sea unless more SDD maps are estimated from other Landsat-TM images using the proposed approach.

Limited experiments in modeling SST show the potential of predicting SST from the thermal channel (6) of Landsat-TM data using a simple linear regression. However, if the calibration data is multi-date, the data should be de-centered (mean removed) to achieve better calibration because SST varies quite significantly from season to season.

## ACKNOWLEDGEMENTS

The Institute of Lowland Technology and the Department of Civil Engineering of Saga University funded this study and the first author during his sabbatical leave from the University of Alberta, Canada. Saga and Kumamoto Prefectures collected the field data and the National Space Development Agency of Japan prepared the Landsat-TM images. The authors gratefully thank Mr. Kato of Saga University for preparing the figures.

## REFERENCES

Abiodun, A. A. (1976). Satellite survey of particulate distribution patterns in Lake Kainji. Remote Sensing of Environ. 5: 109-123.

Abiodun, A. A., and Adeniji, H. (1978). Movement of water columns in Lake Kainji. Remote Sensing of Environ. 7: 227-234.

Aranuvachapun, S., and P. H. LeBlond (1984). Turbidity of coastal water determined from Landsat. Remote Sensing of Environ. 14: 113–132.

Austin, R. W., (1974). The remote sensing of spectral radiance from below the ocean surface. Optical Aspects of Oceanography. Academic London: 317-344.

Bagheri, S., and Dios, R. (1990). Chlorophyll-a estimation in New Jersey's coastal waters using Thematic Mapper data. Int. J. Remote Sensing. 11: 289-299.

Biftu, G. F., and Gan, T. Y. (1999). Retrieving soil moisture from Radarsat SAR data. Water Resources Research. 35(5): 1569-1579, American Geophysical Union.

Carpenter, D. J., and S. M. Carpenter (1983). Modeling inland water quality using Landsat data. Remote Sensing of Environ. 13: 345–352.

Caselles, V., and M. J. Lopez Garcia (1989). An alternative simple approach to estimate atmospheric correction in multitemporal studies. Int. J. Remote Sensing. 10(6): 1127-1134.

Duan Q., Sorooshian S., and Gupta V. K. (1992). Effective and efficient global optimization for conceptual rainfall runoff models. Water Resources Research. 28(4): 1015 - 1031.

Duguay, C. R., and LeDrew, E. F. (1991). Mapping surface albedo in the east slope of the Colorado Front Range, USA, with Landsat Thematic Mapper. Arctic and Alpine Research. 23: 213-223.

Engman, E. T., and R. J. Gurney (1991). Remote Sensing in Hydrology. Chapman and Hall.

Gan,T. Y. and G. F. Biftu (1996). Automatic calibration of conceptual rainfall-runoff models: optimization algorithms, catchment conditions, and model structure. Water Resources Res. AGU, Dec. 32(12): 3513-3524.

Gibbons, D. E., Wukelic, G. E., Leighton, J. P., and Doyle, M. J. (1989). Application of Landsat Thematic Mapper data for coastal thermal plume analysis at Diablo Canyon. Photogrammetric Engineering and Remote Sensing. 55: 903-909.

Han, L., Rundquist, D.C., Liu, L. L., Fraser, R. N., and Schalles, J. F. (1984). The spectral responses of algal chlorophyll in water with varying levels of suspended sediment. Int. J. Remote Sensing. 15(18): 3707–3718.

Hovis, W. A., and Leung, K. C. (1977). Remote sensing of ocean color. Opt. Eng. 16(2): 158–166.

Khorram, S. (1985). Development of water quality models applicable throughout the entire San Francisco Bay and delta. Photogram. Eng. Remote Sensing. 51: 53–62.

Kneizys, F. X., Shettle, E. P., Abreu, L. W., Chetwynd, J. H., Anderson, G. P., Gallery, W. O., Selby, J. E. A., and Clough, S. A. (1988). User code to LOWTRAN 7. AFGL-TR-88-0177 Environmental Research papers. No. 1010. US Department of Defense, Air Force Geophysics Laboratory. Optical Physics Division. 137.

Mizuo H., et al. (1998). Water Quality Monitoring by Satellite Remote Sensing Data, An Introduction of Tokyo Bay Project by Some Members of Self Governing Body. Journal of the Remote Sensing Society of Japan. 18(3): 62-66.

Nelder J. A., and Mead R. (1965). A simplex method for functional minimization. Computer Journal. 9: 308-313.

Pattiaratchi, C., P. Lavery, A. Wyllie, and P. T. Hick (1991). Remote sensing in Cockburn Sound: development of water quality algorithms and applicability to monitoring. U. Western Australia Centre for Water Research. Report # ED 607.

Pattiaratchi, C., P. Lavery, A. Wyllie, and P. T. Hick (1994). Estimates of water quality in coastal waters using multi-date Lansat Thematic Mapper Data. Int. J. Remote Sensing. 15(8): 1571–1584.

Price, J. (1983). Estimating surface temperatures from satellite thermal infrared data–a simple formulation for the atmospheric effect. Remote Sensing of Environ. 13: 353-361.

Reid, G. K. (1965). Ecology of Inland Waters and Estuaries. 4th edn. Reinhold, New York.

Richter, R. (1991). Error bounds of a fast atmospheric correction algorithm for the Landsat thematic mapper and multispectral scanner bands. Applied Optics: 30(30): 4412–4417.

Ritchie, J. C., F. R. Schiebe, and C. M. Cooper (1984). Use of Landsat TM data to monitor suspended sediments in agricultural impoundments. Proceedings 3rd Australasian Remote Sensing Conf. Queensland. Australia. Organizing Committee Landsat 84, Brisbane, Australia, 79-87.

Schott, J. R. and Volchok, W.J. (1985). Thematic Mapper Thermal Infrared Calibration. Photogrammetric Engineering and Remote Sensing. 51(9): 1351-1357.

Seguchi, M. and K. Watanabe (1989). Study on oceanic phenomena in the shallow area of the Ariake Sea by remote sensing, III–estimated distributions of turbidity and sea surface temperature by Landsat-5 TM data. Bull. Fac. Agr. Saga University. 66: 77-83. Saga, Japan.

Singh, A. (1989). Review article–digital change detection techniques using remotely sensed data. Int. J. Remote Sensing. 10: 989–1003.

Singh, P.S., and Gan, T.Y. (1999). Estimation of Snow Water Equivalent Using Passive Microwave Brightness Temperature Data. submitted to Remote Sensing of Environment, Elsevier Science.

Tassan, S. (1987). Evaluation of the potential of the Thematic Mapper for Marine application, Int. J. Remote Sensing. 8: 1455–1478.

Thomas, I. L. (1980). Suspended sediment dynamics from repetitive Landsat data. Int. J. Remote Sensing. 1(3): 285-292.

Watanabe, K. and M. Seguchi, (1987). Study on oceanic phenomena in the shallow area of Ariake Sea by remote sensing, I, Bull. Fac. Agr. Saga University. 63: 55-64. Saga, Japan.

Watanabe, K. and M., Seguchi (1988). Study on oceanic phenomena in the shallow area of Ariake Sea by remote sensing, II, Observation of flow regime by Landsat 5 TM data, Bull. Fac. Agr. Saga University. 65: 53-59. Saga, Japan.